First study of the radiation-amplitude zero in $W\gamma$ production and limits on anomalous $WW\gamma$ couplings at $\sqrt{s} = 1.96$ TeV

V.M. Abazov[36], B. Abbott[75], M. Abolins[65], B.S. Acharya[29], M. Adams[51], T. Adams[49], E. Aguilo[6], S.H. Ahn[31], M. Ahsan[59], G.D. Alexeev[36], G. Alkhazov[40], A. Alton[64,a], G. Alverson[63], G.A. Alves[2], M. Anastasoaie[35], L.S. Ancu[35], T. Andeen[53], S. Anderson[45], B. Andrieu[17], M.S. Anzelc[53], M. Aoki[50], Y. Arnoud[14], M. Arov[60], M. Arthaud[18], A. Askew[49], B. Åsman[41], A.C.S. Assis Jesus[3], O. Atramentov[49], C. Avila[8], C. Ay[24], F. Badaud[13], A. Baden[61], L. Bagby[50], B. Baldin[50], D.V. Bandurin[59], P. Banerjee[29], S. Banerjee[29], E. Barberis[63], A.-F. Barfuss[15], P. Bargassa[80], P. Baringer[58], J. Barreto[2], J.F. Bartlett[50], U. Bassler[18], D. Bauer[43], S. Beale[6], A. Bean[58], M. Begalli[3], M. Begel[73], C. Belanger-Champagne[41], L. Bellantoni[50], A. Bellavance[50], J.A. Benitez[65], S.B. Beri[27], G. Bernardi[17], R. Bernhard[23], I. Bertram[42], M. Besançon[18], R. Beuselinck[43], V.A. Bezzubov[39], P.C. Bhat[50], V. Bhatnagar[27], C. Biscarat[20], G. Blazey[52], F. Blekman[43], S. Blessing[49], D. Bloch[19], K. Bloom[67], A. Boehnlein[50], D. Boline[62], T.A. Bolton[59], G. Borissov[42], T. Bose[77], A. Brandt[78], R. Brock[65], G. Brooijmans[70], A. Bross[50], D. Brown[81], N.J. Buchanan[49], D. Buchholz[53], M. Buehler[81], V. Buescher[22], V. Bunichev[38], S. Burdin[42,b], S. Burke[45], T.H. Burnett[82], C.P. Buszello[43], J.M. Butler[62], P. Calfayan[25], S. Calvet[16], J. Cammin[71], W. Carvalho[3], B.C.K. Casey[50], H. Castilla-Valdez[33], S. Chakrabarti[18], D. Chakraborty[52], K. Chan[6], K.M. Chan[55], A. Chandra[48], F. Charles[19,‡], E. Cheu[45], F. Chevallier[14], D.K. Cho[62], S. Choi[32], B. Choudhary[28], L. Christofek[77], T. Christoudias[43], S. Cihangir[50], D. Claes[67], Y. Coadou[6], M. Cooke[80], W.E. Cooper[50], M. Corcoran[80], F. Couderc[18], M.-C. Cousinou[15], S. Crépé-Renaudin[14], D. Cutts[77], M. Ćwiok[30], H. da Motta[2], A. Das[45], G. Davies[43], K. De[78], S.J. de Jong[35], E. De La Cruz-Burelo[64], C. De Oliveira Martins[3], J.D. Degenhardt[64], F. Déliot[18], M. Demarteau[50], R. Demina[71], D. Denisov[50], S.P. Denisov[39], S. Desai[50], H.T. Diehl[50], M. Diesburg[50], A. Dominguez[67], H. Dong[72], L.V. Dudko[38], L. Duflot[16], S.R. Dugad[29], D. Duggan[49], A. Duperrin[15], J. Dyer[65], A. Dyshkant[52], M. Eads[67], D. Edmunds[65], J. Ellison[48], V.D. Elvira[50], Y. Enari[77], S. Eno[61], P. Ermolov[38], H. Evans[54], A. Evdokimov[73], V.N. Evdokimov[39], A.V. Ferapontov[59], T. Ferbel[71], F. Fiedler[24], F. Filthaut[35], W. Fisher[50], H.E. Fisk[50], M. Fortner[52], H. Fox[42], S. Fu[50], S. Fuess[50], T. Gadfort[70], C.F. Galea[35], E. Gallas[50], C. Garcia[71], A. Garcia-Bellido[82], V. Gavrilov[37], P. Gay[13], W. Geist[19], D. Gelé[19], C.E. Gerber[51], Y. Gershtein[49], D. Gillberg[6], G. Ginther[71], N. Gollub[41], B. Gómez[8], A. Goussiou[82], P.D. Grannis[72], H. Greenlee[50], Z.D. Greenwood[60], E.M. Gregores[4], G. Grenier[20], Ph. Gris[13], J.-F. Grivaz[16], A. Grohsjean[25], S. Grünendahl[50], M.W. Grünewald[30], F. Guo[72], J. Guo[72], G. Gutierrez[50], P. Gutierrez[75], A. Haas[70], N.J. Hadley[61], P. Haefner[25], S. Hagopian[49], J. Haley[68], I. Hall[65], R.E. Hall[47], L. Han[7], K. Harder[44], A. Harel[71], R. Harrington[63], J.M. Hauptman[57], R. Hauser[65], J. Hays[43], T. Hebbeker[21], D. Hedin[52], J.G. Hegeman[34], J.M. Heinmiller[51], A.P. Heinson[48], U. Heintz[62], C. Hensel[58], K. Herner[72], G. Hesketh[63], M.D. Hildreth[55], R. Hirosky[81], J.D. Hobbs[72], B. Hoeneisen[12], H. Hoeth[26], M. Hohlfeld[22], S.J. Hong[31], S. Hossain[75], P. Houben[34], Y. Hu[72], Z. Hubacek[10], V. Hynek[9], I. Iashvili[69], R. Illingworth[50], A.S. Ito[50], S. Jabeen[62], M. Jaffré[16], S. Jain[75], K. Jakobs[23], C. Jarvis[61], R. Jesik[43], K. Johns[45], C. Johnson[70], M. Johnson[50], A. Jonckheere[50], P. Jonsson[43], A. Juste[50], E. Kajfasz[15], A.M. Kalinin[36], J.M. Kalk[60], S. Kappler[21], D. Karmanov[38], P.A. Kasper[50], I. Katsanos[70], D. Kau[49], V. Kaushik[78], R. Kehoe[79], S. Kermiche[15], N. Khalatyan[50], A. Khanov[76], A. Kharchilava[69], Y.M. Kharzheev[36], D. Khatidze[70], T.J. Kim[31], M.H. Kirby[53], M. Kirsch[21], B. Klima[50], J.M. Kohli[27], J.-P. Konrath[23], V.M. Korablev[39], A.V. Kozelov[39], J. Kraus[65], D. Krop[54], T. Kuhl[24], A. Kumar[69], A. Kupco[11], T. Kurča[20], J. Kvita[9], F. Lacroix[13], D. Lam[55], S. Lammers[70], G. Landsberg[77], P. Lebrun[20], W.M. Lee[50], A. Leflat[38], J. Lellouch[17], J. Leveque[45], J. Li[78], L. Li[48], Q.Z. Li[50], S.M. Lietti[5], J.G.R. Lima[52], D. Lincoln[50], J. Linnemann[65], V.V. Lipaev[39], R. Lipton[50], Y. Liu[7], Z. Liu[6], A. Lobodenko[40], M. Lokajicek[11], P. Love[42], H.J. Lubatti[82], R. Luna[3], A.L. Lyon[50], A.K.A. Maciel[2], D. Mackin[80], R.J. Madaras[46], P. Mättig[26], C. Magass[21], A. Magerkurth[64], P.K. Mal[82], H.B. Malbouisson[3], S. Malik[67], V.L. Malyshev[36], H.S. Mao[50], Y. Maravin[59], B. Martin[14], R. McCarthy[72], A. Melnitchouk[66], L. Mendoza[8], P.G. Mercadante[5], M. Merkin[38], K.W. Merritt[50], A. Meyer[21], J. Meyer[22,d], T. Millet[20], J. Mitrevski[70], J. Molina[3], R.K. Mommsen[44], N.K. Mondal[29], R.W. Moore[6], T. Moulik[58], G.S. Muanza[20], M. Mulders[50], M. Mulhearn[70], O. Mundal[22], L. Mundim[3], E. Nagy[15], M. Naimuddin[50], M. Narain[77], N.A. Naumann[35], H.A. Neal[64], J.P. Negret[8], P. Neustroev[40], H. Nilsen[23], H. Nogima[3], S.F. Novaes[5], T. Nunnemann[25], V. O'Dell[50], D.C. O'Neil[6], G. Obrant[40], C. Ochando[16], D. Onoprienko[59], N. Oshima[50], N. Osman[43], J. Osta[55], R. Otec[10], G.J. Otero y Garzón[50], M. Owen[44], P. Padley[80], M. Pangilinan[77], N. Parashar[56], S.-J. Park[71], S.K. Park[31], J. Parsons[70], R. Partridge[77], N. Parua[54], A. Patwa[73], G. Pawloski[80], B. Penning[23], M. Perfilov[38], K. Peters[44],

Y. Peters[26], P. Pétroff[16], M. Petteni[43], R. Piegaia[1], J. Piper[65], M.-A. Pleier[22], P.L.M. Podesta-Lerma[33,c], V.M. Podstavkov[50], Y. Pogorelov[55], M.-E. Pol[2], P. Polozov[37], B.G. Pope[65], A.V. Popov[39], C. Potter[6], W.L. Prado da Silva[3], H.B. Prosper[49], S. Protopopescu[73], J. Qian[64], A. Quadt[22,d], B. Quinn[66], A. Rakitine[42], M.S. Rangel[2], K. Ranjan[28], P.N. Ratoff[42], P. Renkel[79], S. Reucroft[63], P. Rich[44], J. Rieger[54], M. Rijssenbeek[72], I. Ripp-Baudot[19], F. Rizatdinova[76], S. Robinson[43], R.F. Rodrigues[3], M. Rominsky[75], C. Royon[18], P. Rubinov[50], R. Ruchti[55], G. Safronov[37], G. Sajot[14], A. Sánchez-Hernández[33], M.P. Sanders[17], A. Santoro[3], G. Savage[50], L. Sawyer[60], T. Scanlon[43], D. Schaile[25], R.D. Schamberger[72], Y. Scheglov[40], H. Schellman[53], T. Schliephake[26], C. Schwanenberger[44], A. Schwartzman[68], R. Schwienhorst[65], J. Sekaric[49], H. Severini[75], E. Shabalina[51], M. Shamim[59], V. Shary[18], A.A. Shchukin[39], R.K. Shivpuri[28], V. Siccardi[19], V. Simak[10], V. Sirotenko[50], P. Skubic[75], P. Slattery[71], D. Smirnov[55], G.R. Snow[67], J. Snow[74], S. Snyder[73], S. Söldner-Rembold[44], L. Sonnenschein[17], A. Sopczak[42], M. Sosebee[78], K. Soustruznik[9], B. Spurlock[78], J. Stark[14], J. Steele[60], V. Stolin[37], D.A. Stoyanova[39], J. Strandberg[64], S. Strandberg[41], M.A. Strang[69], E. Strauss[72], M. Strauss[75], R. Ströhmer[25], D. Strom[53], L. Stutte[50], S. Sumowidagdo[49], P. Svoisky[55], A. Sznajder[3], P. Tamburello[45], A. Tanasijczuk[1], W. Taylor[6], J. Temple[45], B. Tiller[25], F. Tissandier[13], M. Titov[18], V.V. Tokmenin[36], T. Toole[61], I. Torchiani[23], T. Trefzger[24], D. Tsybychev[72], B. Tuchming[18], C. Tully[68], P.M. Tuts[70], R. Unalan[65], L. Uvarov[40], S. Uvarov[40], S. Uzunyan[52], B. Vachon[6], P.J. van den Berg[34], R. Van Kooten[54], W.M. van Leeuwen[34], N. Varelas[51], E.W. Varnes[45], I.A. Vasilyev[39], M. Vaupel[26], P. Verdier[20], L.S. Vertogradov[36], M. Verzocchi[50], F. Villeneuve-Seguier[43], P. Vint[43], P. Vokac[10], E. Von Toerne[59], M. Voutilainen[68,e], R. Wagner[68], H.D. Wahl[49], L. Wang[61], M.H.L.S. Wang[50], J. Warchol[55], G. Watts[82], M. Wayne[55], G. Weber[24], M. Weber[50], L. Welty-Rieger[54], A. Wenger[23,f], N. Wermes[22], M. Wetstein[61], A. White[78], D. Wicke[26], G.W. Wilson[58], S.J. Wimpenny[48], M. Wobisch[60], D.R. Wood[63], T.R. Wyatt[44], Y. Xie[77], S. Yacoob[53], R. Yamada[50], M. Yan[61], T. Yasuda[50], Y.A. Yatsunenko[36], K. Yip[73], H.D. Yoo[77], S.W. Youn[53], J. Yu[78], A. Zatserklyaniy[52], C. Zeitnitz[26], T. Zhao[82], B. Zhou[64], J. Zhu[72], M. Zielinski[71], D. Zieminska[54], A. Zieminski[54,‡], L. Zivkovic[70], V. Zutshi[52], and E.G. Zverev[38]

(The DØ Collaboration)

[1] *Universidad de Buenos Aires, Buenos Aires, Argentina*
[2] *LAFEX, Centro Brasileiro de Pesquisas Físicas, Rio de Janeiro, Brazil*
[3] *Universidade do Estado do Rio de Janeiro, Rio de Janeiro, Brazil*
[4] *Universidade Federal do ABC, Santo André, Brazil*
[5] *Instituto de Física Teórica, Universidade Estadual Paulista, São Paulo, Brazil*
[6] *University of Alberta, Edmonton, Alberta, Canada, Simon Fraser University, Burnaby, British Columbia, Canada, York University, Toronto, Ontario, Canada, and McGill University, Montreal, Quebec, Canada*
[7] *University of Science and Technology of China, Hefei, People's Republic of China*
[8] *Universidad de los Andes, Bogotá, Colombia*
[9] *Center for Particle Physics, Charles University, Prague, Czech Republic*
[10] *Czech Technical University, Prague, Czech Republic*
[11] *Center for Particle Physics, Institute of Physics, Academy of Sciences of the Czech Republic, Prague, Czech Republic*
[12] *Universidad San Francisco de Quito, Quito, Ecuador*
[13] *LPC, Univ Blaise Pascal, CNRS/IN2P3, Clermont, France*
[14] *LPSC, Université Joseph Fourier Grenoble 1, CNRS/IN2P3, Institut National Polytechnique de Grenoble, France*
[15] *CPPM, IN2P3/CNRS, Université de la Méditerranée, Marseille, France*
[16] *LAL, Univ Paris-Sud, IN2P3/CNRS, Orsay, France*
[17] *LPNHE, IN2P3/CNRS, Universités Paris VI and VII, Paris, France*
[18] *DAPNIA/Service de Physique des Particules, CEA, Saclay, France*
[19] *IPHC, Université Louis Pasteur et Université de Haute Alsace, CNRS/IN2P3, Strasbourg, France*
[20] *IPNL, Université Lyon 1, CNRS/IN2P3, Villeurbanne, France and Université de Lyon, Lyon, France*
[21] *III. Physikalisches Institut A, RWTH Aachen, Aachen, Germany*
[22] *Physikalisches Institut, Universität Bonn, Bonn, Germany*
[23] *Physikalisches Institut, Universität Freiburg, Freiburg, Germany*
[24] *Institut für Physik, Universität Mainz, Mainz, Germany*
[25] *Ludwig-Maximilians-Universität München, München, Germany*
[26] *Fachbereich Physik, University of Wuppertal, Wuppertal, Germany*
[27] *Panjab University, Chandigarh, India*
[28] *Delhi University, Delhi, India*

[29] *Tata Institute of Fundamental Research, Mumbai, India*
[30] *University College Dublin, Dublin, Ireland*
[31] *Korea Detector Laboratory, Korea University, Seoul, Korea*
[32] *SungKyunKwan University, Suwon, Korea*
[33] *CINVESTAV, Mexico City, Mexico*
[34] *FOM-Institute NIKHEF and University of Amsterdam/NIKHEF, Amsterdam, The Netherlands*
[35] *Radboud University Nijmegen/NIKHEF, Nijmegen, The Netherlands*
[36] *Joint Institute for Nuclear Research, Dubna, Russia*
[37] *Institute for Theoretical and Experimental Physics, Moscow, Russia*
[38] *Moscow State University, Moscow, Russia*
[39] *Institute for High Energy Physics, Protvino, Russia*
[40] *Petersburg Nuclear Physics Institute, St. Petersburg, Russia*
[41] *Lund University, Lund, Sweden, Royal Institute of Technology and Stockholm University, Stockholm, Sweden, and Uppsala University, Uppsala, Sweden*
[42] *Lancaster University, Lancaster, United Kingdom*
[43] *Imperial College, London, United Kingdom*
[44] *University of Manchester, Manchester, United Kingdom*
[45] *University of Arizona, Tucson, Arizona 85721, USA*
[46] *Lawrence Berkeley National Laboratory and University of California, Berkeley, California 94720, USA*
[47] *California State University, Fresno, California 93740, USA*
[48] *University of California, Riverside, California 92521, USA*
[49] *Florida State University, Tallahassee, Florida 32306, USA*
[50] *Fermi National Accelerator Laboratory, Batavia, Illinois 60510, USA*
[51] *University of Illinois at Chicago, Chicago, Illinois 60607, USA*
[52] *Northern Illinois University, DeKalb, Illinois 60115, USA*
[53] *Northwestern University, Evanston, Illinois 60208, USA*
[54] *Indiana University, Bloomington, Indiana 47405, USA*
[55] *University of Notre Dame, Notre Dame, Indiana 46556, USA*
[56] *Purdue University Calumet, Hammond, Indiana 46323, USA*
[57] *Iowa State University, Ames, Iowa 50011, USA*
[58] *University of Kansas, Lawrence, Kansas 66045, USA*
[59] *Kansas State University, Manhattan, Kansas 66506, USA*
[60] *Louisiana Tech University, Ruston, Louisiana 71272, USA*
[61] *University of Maryland, College Park, Maryland 20742, USA*
[62] *Boston University, Boston, Massachusetts 02215, USA*
[63] *Northeastern University, Boston, Massachusetts 02115, USA*
[64] *University of Michigan, Ann Arbor, Michigan 48109, USA*
[65] *Michigan State University, East Lansing, Michigan 48824, USA*
[66] *University of Mississippi, University, Mississippi 38677, USA*
[67] *University of Nebraska, Lincoln, Nebraska 68588, USA*
[68] *Princeton University, Princeton, New Jersey 08544, USA*
[69] *State University of New York, Buffalo, New York 14260, USA*
[70] *Columbia University, New York, New York 10027, USA*
[71] *University of Rochester, Rochester, New York 14627, USA*
[72] *State University of New York, Stony Brook, New York 11794, USA*
[73] *Brookhaven National Laboratory, Upton, New York 11973, USA*
[74] *Langston University, Langston, Oklahoma 73050, USA*
[75] *University of Oklahoma, Norman, Oklahoma 73019, USA*
[76] *Oklahoma State University, Stillwater, Oklahoma 74078, USA*
[77] *Brown University, Providence, Rhode Island 02912, USA*
[78] *University of Texas, Arlington, Texas 76019, USA*
[79] *Southern Methodist University, Dallas, Texas 75275, USA*
[80] *Rice University, Houston, Texas 77005, USA*
[81] *University of Virginia, Charlottesville, Virginia 22901, USA and*
[82] *University of Washington, Seattle, Washington 98195, USA*

(Dated: February 29, 2008)

We present results from a study of $p\bar{p} \to W\gamma + X$ events utilizing data corresponding to 0.7 fb^{-1} of integrated luminosity at $\sqrt{s} = 1.96$ TeV collected by the D0 detector at the Fermilab Tevatron Collider. We set limits on anomalous $WW\gamma$ couplings at the 95% C.L. The one dimensional 95% C.L. limits are $0.49 < \kappa_\gamma < 1.51$ and $-0.12 < \lambda_\gamma < 0.13$. We make the first study of the charge-signed rapidity difference between the lepton and the photon and find it to be indicative of the standard model radiation-amplitude zero in the $W\gamma$ system.

PACS numbers: 12.15.Ji, 13.40.Em, 13.85.Qk

Self-interactions of the electroweak bosons are a consequence of the $SU(2)_L \times U(1)_Y$ gauge symmetry of the standard model (SM). In this Letter, we investigate the $WW\gamma$ vertex by studying the production of $p\bar{p} \to W\gamma \to \ell\nu\gamma + X$ events where ℓ is an electron or a muon. At leading order (LO), the SM allows $q\bar{q}' \to W\gamma$ production in which a photon radiates off an incoming quark (initial state radiation) or is directly produced from the $WW\gamma$ vertex. In the SM, these two cases involve three amplitudes where each alone violates unitarity, but together interfere to give a finite cross section. This interference leads to a radiation-amplitude zero (RAZ) in the angular distribution of the photon. In this Letter, we set limits on non-SM $WW\gamma$ couplings and present a first measurement of the destructive interference indicative of the RAZ in the $W\gamma$ system.

Non-SM $WW\gamma$ couplings will give rise to an increase in the $W\gamma$ production cross section over the SM prediction, particularly for energetic photons. CP-conserving couplings may be parameterized by an effective Lagrangian [1, 2] with two parameters, κ_γ and λ_γ, related to the magnetic dipole and electric quadrupole moments of the W boson. In the SM, $\kappa_\gamma = 1$ and $\lambda_\gamma = 0$. The effective Lagrangian with non-SM couplings will violate unitarity at high energies, and so a form factor with a scale Λ is introduced to modify the coupling parameters with $a_0 \to a_0/(1 + \hat{s}/\Lambda^2)^2$ where $a_0 = \kappa_\gamma, \lambda_\gamma$, and $\sqrt{\hat{s}}$ is the $W\gamma$ invariant mass. We set Λ to 2 TeV [3].

A general consequence of gauge theories is that any four-particle tree amplitude involving one or more massless gauge bosons may be factorized into a charge dependent part and a spin/polarization dependent part. The charge dependent part will lead to the amplitude vanishing at a particular point in phase space. For a $2 \to 2$ process, as is the case for $W\gamma$, this effect is evident as a zero in the production amplitude in the angular distribution of the photon [2]. The RAZ manifests itself as a dip in the charge-signed rapidity difference, $Q_\ell \times \Delta y$, between the photon and the charged lepton from the W boson decay [4]. In the massless limit regime, the rapidity difference can be approximated by the pseudorapidity difference [5], which can be very precisely measured. The SM predicts that the dip minimum depends on the quark electric charges and lies at $Q_\ell \times \Delta\eta \approx -1/3$. In the case of anomalous couplings the location of the dip minimum does not change, instead the dip may become more shallow or disappear entirely.

$W\gamma$ production has been studied previously at hadron colliders [6]. The limits set by the most recent previous DØ analysis represented the most stringent constraints on anomalous $WW\gamma$ couplings obtained by direct observation of $W\gamma$ production. The present analysis uses more than four times as much data as well as photons in the end-cap calorimeter, and thus has an increased sensitivity for the study of $Q_\ell \times \Delta\eta$. The D0 detector [7] is used in this study to observe $p\bar{p} \to \ell\nu\gamma + X$ ($\ell = e$ or μ) in collisions at $\sqrt{s} = 1.96$ TeV at the Fermilab Tevatron collider. The data samples correspond to integrated luminosities of 717 ± 44 pb^{-1} and 662 ± 40 pb^{-1} for the electron and muon channels, respectively.

Candidate events with the W boson decaying into an electron and a neutrino are collected with a suite of single electron triggers. The reconstructed electron is required to be in the central ($|\eta_{\rm det}| < 1.1$) or end-cap ($1.5 < |\eta_{\rm det}| < 2.5$) calorimeters [5], have transverse energy $E_T > 25$ GeV, be isolated in the calorimeter, have a shower shape consistent with that of an electromagnetic object, and match a track reconstructed in the central tracking system. The missing transverse energy, $\not\!\!E_T$, must exceed 25 GeV. To reduce final state radiation of photons from leptons, the reconstructed W transverse mass must exceed 50 GeV/c^2. Furthermore, to suppress background from $Z \to ee$ events with an electron misidentified as a photon, the two-body invariant mass of the electron and photon must be outside the mass window 87-97 GeV/c^2. The optimized window limits are asymmetric about the Z boson mass because the expected signal will have more events below the Z boson mass than above it.

Candidate events with the W boson decaying into a muon and a neutrino are collected with a suite of single muon triggers. The reconstructed muon is required to be within $|\eta_{\rm det}| < 1.6$, isolated in the central tracking system and the calorimeter and be associated with a central track with $p_T > 20$ GeV/c. The event $\not\!\!E_T$ must exceed 20 GeV and there must be no additional isolated tracks with $p_T > 15$ GeV/c as well as no additional muons. The muon momentum is measured by the curvature of the track in the central tracking system.

Photons are identified with the same requirements in both channels. The photon must have $E_T > 9$ GeV and be in the central ($|\eta_{\rm det}| < 1.1$) or end-cap ($1.5 < |\eta_{\rm det}| < 2.5$) calorimeter. It must be isolated in the calorimeter and tracker, have a shower shape consistent with that of an electromagnetic object, have an associated cluster in the preshower detector, and, if in the central region, project back to a position along the beam axis within 10 cm of the primary vertex. The photon and the lepton must be separated in $\eta - \phi$ space by $\Delta R = \sqrt{(\Delta\eta)^2 + (\Delta\phi)^2} > 0.7$. To further suppress final state radiation, the three-body transverse mass (M_{T3}) of the photon, lepton, and missing transverse energy must exceed 120 GeV/c^2 and 110 GeV/c^2 for the electron and muon channels, respectively.

Kinematic and geometric acceptances are determined using Monte Carlo (MC) events. For the acceptances to

TABLE I: Summary of event yields. When uncertainties are shown, the first is statistical and the second is systematic. When only one uncertainty is shown, it is systematic.

	$e\nu\gamma$ channel	$\mu\nu\gamma$ channel
Luminosity	720 ± 44 pb^{-1}	660 ± 40 pb^{-1}
Acceptance × efficiency	0.063 ± 0.003	0.045 ± 0.003
W + jet background	$34 \pm 3.8 \pm 3.1$	$18 \pm 2.9 \pm 1.9$
ℓeX background	$17 \pm 2.7 \pm 1.3$	$2.7 \pm 1.3 \pm 0.2$
$W \to \tau$ background	$1.1 \pm 0.1 \pm 0.1$	$1.4 \pm 0.2 \pm 0.1$
$Z\gamma$ background	—	$3.8 \pm 0.53 \pm 0.42$
Candidate events	180	83
Measured signal	$130 \pm 14 \pm 3.4$	$57 \pm 8.8 \pm 1.8$
SM prediction	120 ± 12	77 ± 9.4

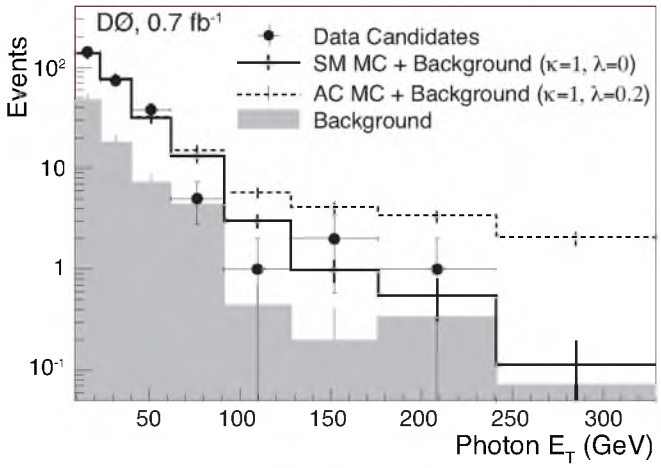

FIG. 1: The photon transverse energy spectra for the SM (solid line), an anomalous coupling (AC) point (dashed line), combined electron and muon channel data candidates (black points), and the background estimate (shaded histogram). Uncertainties are shown as error bars on the points, lines, and histograms. The last bin includes overflows.

be meaningful, they are measured with respect to reference kinematic requirements of $E_T^\gamma > 9$ GeV, $M_{T3} > 90$ GeV/c^2, and $\Delta R > 0.7$ (MC samples were produced with much looser requirements). A LO simulation [8] of $W\gamma$ production is used, which includes the contributions from initial and final state radiation as well as the $WW\gamma$ trilinear vertex. To compensate for the effects of next-to-leading order (NLO) corrections on the E_T^γ spectrum, a NLO MC [9] is used, and an E_T^γ-dependent K-factor is calculated and applied to the LO spectra. The detector resolutions are applied using a parameterized simulation.

Electron and muon identification efficiencies are determined with large $Z \to ee$ or $Z \to \mu\mu$ samples from the data. The photon detection efficiency is determined by the full GEANT [10] detector simulation and is verified with $Z\gamma$ data. In these events, the photon is radiated from a final state lepton and so the three-body mass of the photon and the leptons should reconstruct the Z boson mass. The reconstruction efficiency from the GEANT MC is scaled to match the measured efficiency from the $Z\gamma$ process in data. The acceptance times efficiency values described here are shown in Table I.

Backgrounds to $W\gamma$ production include W + jet events where the jet is misidentified as a photon; "ℓeX" events with a lepton, electron, and $\not\!\!E_T$ where the electron is misidentified as a photon; $Z\gamma \to \ell\ell\gamma$ events where a lepton is lost; and $W\gamma \to \tau\nu\gamma$. The W + jet background dominates both channels and is determined from data. The rate at which a jet is misidentified as a photon is calculated from a large multijet sample in which the jets under study are required to have a large fraction of their energy deposited in the electromagnetic layers of the calorimeter. This rate is calculated as a function of E_T and $\eta_{\rm det}$. The rate is then applied to a normalization sample of W + jet events where the jets satisfy the same criteria as in the multijet sample. To determine the ℓeX background, the track isolation requirement is removed from the photon and a matched track is required. The measured tracking efficiencies are then used to estimate this background contribution. The $Z\gamma$ and $W\gamma \to \tau\nu\gamma \to e(\mu)\nu\nu\gamma$ backgrounds are estimated from MC. The $Q_\ell \times \Delta\eta$ distribution of the total background lacks any statistically significant structure. A summary of the background estimates and the observed $W\gamma$ candidate events are shown in Table I.

Since the observed event yields are consistent with the SM predictions, limits on anomalous $WW\gamma$ trilinear couplings are determined using the combined E_T^γ spectrum from both channels (Fig. 1). Limits are set by generating E_T^γ spectra for different values of the coupling parameters κ_γ and λ_γ, and then calculating the likelihood they represent the data. The 95% C.L. limit contour is found numerically by integrating the likelihood surface and finding the minimum contour that represents 95% of the volume. One-dimensional 95% C.L. limits are calculated by setting one coupling parameter to the SM value and allowing the other to vary. These limits, shown in Fig. 2, are $0.49 < \kappa_\gamma < 1.51$ and $-0.12 < \lambda_\gamma < 0.13$.

The background-subtracted $Q_\ell \times \Delta\eta$ distribution for the combined electron and muon channels is shown in Fig. 3. To perform a statistical test for the presence of a dip, the distribution is divided into two bins whose edges are determined by the $Q_\ell \times \Delta\eta$ distribution generated in SM Monte Carlo. The bins are chosen to be adjacent and of equal width such that one samples the majority of events in the dip and the other samples the smaller of the local maxima (see the inset in Fig. 4). We define a test statistic R to be the ratio of the integral number of events in the dip bin to the integral number of events in the maximum bin. This ratio will be at least one if there is no dip (unimodal distribution), and less than one if there is a dip. For the combined background-subtracted data $Q_\ell \times \Delta\eta$, this ratio test gives a value of 0.64.

We first compare this observed R value from the data

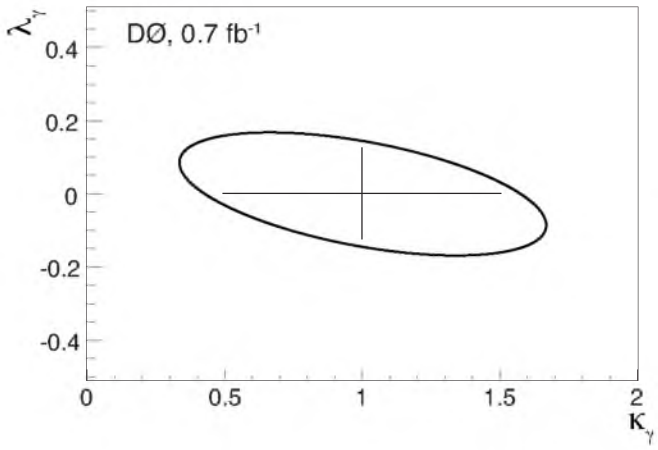

FIG. 2: The ellipse is the 95% C.L. limit contour in $\kappa_\gamma - \lambda_\gamma$ space. One-dimensional 95% C.L. limits are shown as the horizontal and vertical bars.

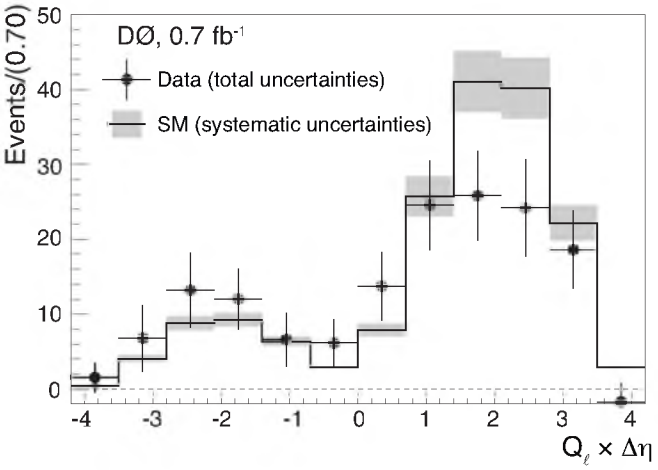

FIG. 3: The background-subtracted charge-signed rapidity difference for the combined electron and muon channels. The black points and error bars represent background-subtracted data with its associated uncertainties (statistical and from the subtraction procedure), and the shaded areas are the systematic uncertainties on the SM prediction (including on efficiencies and acceptances). The solid line is the distribution from the SM. A χ^2 test comparing the data and SM using the full covariance matrix yields 17 for 12 degrees of freedom, indicating good agreement.

to an ensemble of 10^4 MC SM pseudo-experiments where all statistical and systematic fluctuations are included. For the SM, 28% of the experiments have a ratio of 0.64 or greater. In order to evaluate the significance of the observed data R value, we select an anomalous coupling value which provides a $Q_\ell \times \Delta\eta$ distribution that minimally exhibits no dip — the minimal unimodal hypothesis (MUH). Minimal specifically means a class of distributions on the boundary of bimodal and unimodal distributions. The distribution chosen here corresponds to $\kappa_\gamma = 0$, $\lambda_\gamma = -1$ (zero magnetic dipole moment of the

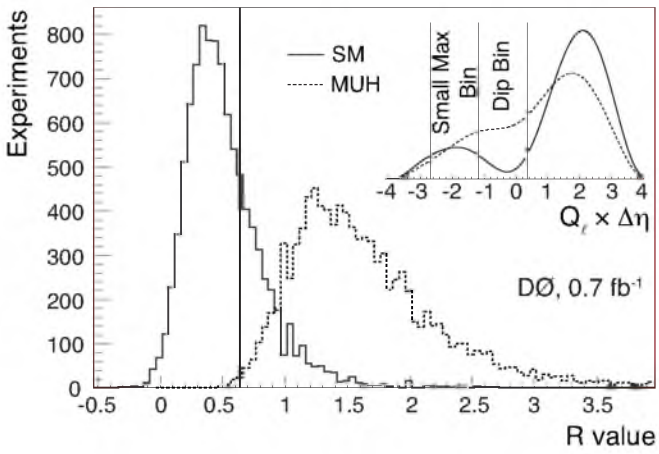

FIG. 4: Distributions of the R-test statistic for the SM ensembles (solid line) and the MUH ensembles (dashed line). The vertical line indicates the measured value from the data. The inset plot indicates the positions of the two bins used for the R-test as determined by a fit to the SM $Q_\ell \times \Delta\eta$ distribution (solid line). For comparison, a fit to the MUH $Q_\ell \times \Delta\eta$ distribution is shown as the dashed line.

W boson). Anomalous couplings increase the event yield as well, but since we are only concerned with the distribution shape, we normalize this distribution to the number of events predicted by the SM. For this MUH case, only 45 experiments out of 10^4 have an R value of 0.64 or smaller due to a random fluctuation. These distributions are shown in Fig. 4. If transformed into a Gaussian significance, this probability corresponds to 2.6σ. This result is the first study of the $Q_\ell \times \Delta\eta$ distribution and is indicative of the RAZ in $W\gamma$ production.

In summary, we have studied $W\gamma$ production and set 95% C.L. limits on anomalous trilinear gauge couplings at $0.49 < \kappa_\gamma < 1.51$ and $-0.12 < \lambda_\gamma < 0.13$. These limits are the most stringent set at a hadron collider for this final state. We also performed the first study of the radiation-amplitude zero in the charge-signed rapidity difference between the lepton and the photon. The probability that this measurement would arise from a minimal unimodal hypothesis is smaller than $(4.5 \pm 0.7) \times 10^{-3}$ and is indicative of the radiation-amplitude zero in $W\gamma$ production.

We thank Prof. David W. Scott, Department of Statistics, Rice University. We thank the staffs at Fermilab and collaborating institutions, and acknowledge support from the DOE and NSF (USA); CEA and CNRS/IN2P3 (France); FASI, Rosatom and RFBR (Russia); CNPq, FAPERJ, FAPESP and FUNDUNESP (Brazil); DAE and DST (India); Colciencias (Colombia); CONACyT (Mexico); KRF and KOSEF (Korea); CONICET and UBACyT (Argentina); FOM (The Netherlands); STFC (United Kingdom); MSMT and GACR (Czech Republic); CRC Program, CFI, NSERC and WestGrid Project (Canada); BMBF and DFG (Germany); SFI (Ireland);

The Swedish Research Council (Sweden); CAS and CNSF (China); and the Alexander von Humboldt Foundation.

---

[a] Visitor from Augustana College, Sioux Falls, SD, USA.
[b] Visitor from The University of Liverpool, Liverpool, UK.
[c] Visitor from ICN-UNAM, Mexico City, Mexico.
[d] Visitor from II. Physikalisches Institut, Georg-August-University, Göttingen, Germany.
[e] Visitor from Helsinki Institute of Physics, Helsinki, Finland.
[f] Visitor from Universität Zürich, Zürich, Switzerland.
[‡] Deceased.

[1] B. Abbott *et al.* (D0 Collaboration), Phys. Rev. D **60**, 072002 (1999).
[2] R. W. Brown, D. Sahdev, and K. O. Mikaelian, Phys. Rev. D **20**, 1164 (1979); K. O. Mikaelian, M. A. Samuel, and D. Sahdev, Phys. Rev. Lett. **43**, 746 (1979); C. J. Goebel, F. Halzen, and J. P. Leveille, Phys. Rev. D **23**, 2682 (1981); S. J. Brodsky and R. W. Brown, Phys. Rev. Lett. **49**, 966 (1982); R. W. Brown, K. L. Kowalski, and S. J. Brodsky, Phys. Rev. D **28**, 624 (1983).
[3] The coupling limits depend on Λ only weakly for $\Lambda > 1$ TeV.
[4] U. Baur, S. Errede, and G. Landsberg, Phys. Rev. D **50**, 1917 (1994).
[5] D0 uses a cylindrical coordinate system with the z axis running along the beam axis. Angles θ and ϕ are the polar and azimuthal angles, respectively. Pseudorapidity is defined as $\eta = -\ln[\tan(\theta/2)]$ where θ is measured with respect to the primary vertex. In the massless limit, η is equivalent to the rapidity $y = (1/2)\ln[(E+p_z)/(E-p_z)]$. $\eta_{\rm det}$ is the pseudorapidity measured with respect to the center of the detector.
[6] V. M. Abazov *et al.* (D0 Collaboration), Phys. Rev. D **71**, 091108(R) (2005); S. Abachi *et al.* (D0 Collaboration), Phys. Rev. Lett. **78**, 3634 (1997); F. Abe *et al.* (CDF Collaboration), Phys. Rev. Lett. **75**, 1017 (1995).
[7] V. M. Abazov *et al.* (D0 Collaboration), Nucl. Instrum. Methods Phys. Res., Sect. A **565**, 463 (2006).
[8] U. Baur and E. L. Berger, Phys. Rev. D **41**, 1476 (1990).
[9] U. Baur, T. Han, and J. Ohnemus, Phys. Rev. D **48**, 5140 (1993). Note that this NLO MC does not include the $W\gamma$ final state radiation process and thus cannot be used to calculate the acceptance directly.
[10] R. Brun and F. Carminati, CERN Program Library Long Writeup W5013, 1993 (unpublished).